Neurobiology of Disease 115 (2018) 157–166

Contents lists available at ScienceDirect

Neurobiology of Disease

journal homepage: www.elsevier.com/locate/ynbdi

A V1143F mutation in the neuronal-enriched isoform 2 of the PMCA pump is linked with ataxia

Mattia Vicario[a,1], Ginevra Zanni[b,1], Francesca Vallese[a], Filippo Santorelli[c], Alessandro Grinzato[a], Domenico Cieri[a], Paola Berto[a], Martina Frizzarin[a], Raffaele Lopreiato[a], Francesco Zonta[d,e], Stefania Ferro[a], Michele Sandre[a], Oriano Marin[a], Maria Ruzzene[a], Enrico Bertini[b], Giuseppe Zanotti[a], Marisa Brini[f,*], Tito Calì[a,g,*], Ernesto Carafoli[h,**]

[a] Department of Biomedical Sciences, University of Padova, 35131 Padova, Italy
[b] Department of Neurosciences, Bambino Gesù Children's Hospital, IRCCS, Rome, Italy
[c] Child Neurology, IRCCS Stella Maris, Pisa, Italy
[d] Shanghai Institute of Advanced Immunochemical Studies, ShanghaiTech University, Shanghai, China
[e] Department of Biomedical Sciences, Institute of Cell Biology and Neurobiology, Italian National Research Council, 00015 Monterotondo, Rome, Italy
[f] Department of Biology, University of Padova, Italy
[g] Padua Neuroscience Center (PNC), University of Padua, 35122 Padova, Italy
[h] Venetian Institute of Molecular Medicine, Padova, Italy

ARTICLE INFO

Keywords:
Calcium signaling
Plasma membrane calcium ATPases
Cerebellar ataxia
Pump mutation

ABSTRACT

The fine regulation of intracellular calcium is fundamental for all eukaryotic cells. In neurons, Ca^{2+} oscillations govern the synaptic development, the release of neurotransmitters and the expression of several genes. Alterations of Ca^{2+} homeostasis were found to play a pivotal role in neurodegenerative progression. The maintenance of proper Ca^{2+} signaling in neurons demands the continuous activity of Ca^{2+} pumps and exchangers to guarantee physiological cytosolic concentration of the cation. The plasma membrane Ca^{2+} ATPases (PMCA pumps) play a key role in the regulation of Ca^{2+} handling in selected sub-plasma membrane microdomains. Among the four basic PMCA pump isoforms existing in mammals, isoforms 2 and 3 are particularly enriched in the nervous system. In humans, genetic mutations in the PMCA2 gene in association with cadherin 23 mutations have been linked to hearing loss phenotypes, while those occurring in the PMCA3 gene were associated with X-linked congenital cerebellar ataxias. Here we describe a novel missense mutation (V1143F) in the calmodulin binding domain (CaM-BD) of the PMCA2 protein. The mutant pump was present in a patient showing congenital cerebellar ataxia but no overt signs of deafness, in line with the absence of mutations in the cadherin 23 gene. Biochemical and molecular dynamics studies on the mutated PMCA2 have revealed that the V1143F substitution alters the binding of calmodulin to the CaM-BD leading to impaired Ca^{2+} ejection.

1. Introduction

The Ca^{2+} ATPase of the plasma membrane (PMCA), a member of the P-type transport ATPases family (Pedersen and Carafoli, 1987), clears Ca^{2+} from the cytosol in cooperation with the Na^{+}/Ca^{2+}exchanger and the SERCA pump, setting the cytosolic Ca^{2+} levels to a physiological range (~100 nM) (Carafoli, 1994). It has a major role as master regulator of Ca^{2+} signaling in selected sub-plasma membrane microdomains (Lopreiato et al., 2014). Its overall structure consists of ten transmembrane domains, two large intracellular loops and a long C-terminal tail containing the calmodulin binding domain (CaM-BD): at resting conditions, the CaMBD inhibits the pump by interacting with its main body, while binding of CaM to its BD activates it in a Ca^{2+}-dependent manner (Falchetto et al., 1991, 1992; Verma et al., 1988). Four distinct genes (*ATP2B1-4*) encode for two ubiquitous (PMCA1 and 4) and two neuron-enriched (PMCA2 and 3) pump isoforms which also differ in distribution at the plasma membrane and functional activity. Numerous variants are further produced by alternative splicing at specific sites in the first cytosolic loop (site A) and within the CaM-BD (site C) of the pump (Strehler and Zacharias, 2001).

* Corresponding authors.
** Correspondence to: E. Carafoli, Venetian Institute of Molecular Medicine, Padova, Italy.
E-mail addresses: marisa.brini@unipd.it (M. Brini), tito.cali@unipd.it (T. Calì), ernesto.carafoli@unipd.it (E. Carafoli).
[1] The authors contributed equally to this work.

https://doi.org/10.1016/j.nbd.2018.04.009
Received 19 February 2018; Received in revised form 21 March 2018; Accepted 9 April 2018
Available online 12 April 2018

In the nervous system, both PMCA2 and PMCA3 concentrate at the cerebellum with PMCA3 mostly associated with the axonal terminal of granule neurons and PMCA2 particularly abundant in dendrites and dendritic spines of Purkinje cells (Filoteo et al., 1997; Hillman et al., 1996). PMCA3 also localizes to the choroid plexus (Eakin et al., 1995) while PMCA2 is also present at the stereocilia of the outer hair cells of the inner ear where it represents the unique Ca^{2+} extrusion system (Dumont et al., 2001). Genetic defects of the neuron-enriched pump isoforms have been linked to precise and specific neuronal disease phenotypes. Those of PMCA2 have been linked to deafness due to the malfunction of the Corti organ of the inner ear (Bortolozzi et al., 2010; Ficarella et al., 2007; Kozel et al., 1998; Schultz et al., 2005; Spiden et al., 2008; Street et al., 1998; Takahashi and Kitamura, 1999; Tsai et al., 2006; Wood et al., 2004) in mice (Spiden et al., 2008; Tsai et al., 2006) and in humans (Ficarella et al., 2007; Schultz et al., 2005). The PMCA2 defects have been found to be accompanied by additional mutations in the stereociliar Ca^{2+} binding protein cadherin 23, indicating a digenic mechanism in the generation of the phenotype. The defects of PMCA3 are associated with X-linked ataxias with cerebellar atrophy both in rat and humans (Cali et al., 2015, 2017; Feyma et al., 2016; Figueroa et al., 2016; Vicario et al., 2017; Zanni et al., 2012). In addition to hearing defects, PMCA2 mutant mice also have motility problems such as unsteady gait, head bobbing and difficulties in maintaining balance (Kozel et al., 1998; Penheiter et al., 2001; Street et al., 1998). Whether this ataxic-like behavior is a consequence of the inner ear defect or can be directly ascribed to cerebellar defects is currently unclear. The PMCA2 presence in the cell bodies, dendrites and dendritic spines Purkinje neurons and its potential role in the clearance of the Ca^{2+} inputs received from parallel fibers (Stahl et al., 1992; Stauffer et al., 1997; Tolosa de Talamoni et al., 1993) suggest a direct involvement of its defects in cerebellar dysfunction and ataxia. However, PMCA2 mutations associated to ataxic phenotypes in the absence of hearing loss have not been reported so far.

In the present study, we have identified a novel missense mutation (V1143F) in the CaM-BD of the PMCA2 pump in the absence of cadherin 23 mutations in a patient affected by congenital cerebellar ataxia but without hearing defects. We have found that the ability of the mutated pump to extrude Ca^{2+} in model cells overexpressing is impaired. Surface plasmon resonance (SPR) analysis of calmodulin interaction with the synthetic CaM-BD and molecular dynamic simulations have also been performed. The results have demonstrated that the mutation interferes with the binding of calmodulin to its CaM-BD.

2. Materials and methods

2.1. Mutation analysis

Targeted next generation sequencing was performed by using standard methods (Qiagen DNA extraction kit) to isolate genomic DNA from peripheral blood of the patient. Informed consent was obtained from the patient. The exonic sequences of genes known to be associated with pediatric ataxia or candidate genes including *ATP2B3* and *ATP2B2*, were analyzed using a Truseq Custom Amplicon (TSCA) (Illumina Inc., San Diego, CA) targeted capture and paired end library kit. Targeted resequencing was performed using TSCA enrichment sequenced on an Illumina MiSEQ desktop sequencer (Illumina Inc.). Selected variants were analyzed using standard pathogenicity prediction programs including PolyPhen-2,16 SIFT,17 and the mutation interpretation software Alamut (http://www.interactive-biosoftware.com/). Sanger sequencing was used to confirm the *ATP2B2* mutation (GenBank accession NM_001001331; ENST00000360273) and to exclude *CDH23* variants (GenBank accession NM_ 022124; ENST00000224721. Segregation analysis could not be performed because of lack of consent from the parents.

2.1.1. Site-direct mutagenesis

The plasmid encoding the z/a and the z/b variants of mutated PMCA2 (V1143F for the canonical full-length protein, V1098F for the z/a and z/b splice variants, herein referred as V1143F) were obtained by site-direct mutagenesis on cDNA templates cloned into pMM2 or pcDNA3 vector, respectively. Mutagenesis were performed using the QuickChange XL site-direct mutagenesis kit (Agilent) by using the following primers: PMCA2 z/a V1143F for, 5′-CAGACACAGATTGAATT CGT CAATACTTTCAAG-3′; rev, 5′-CTTGAAAGTATTGACGAATTCAAT CTGTGTCTG-3′; PMCA2 z/b V1143F for 5′-CCAGACACAGATCCGCTT CGTGAAGGCGTTCCG-3′; rev 5′-CGGAACGCCTTCAC GAAGCGGATCT GTGTCTGG-3′. The constructs were verified by DNA sequencing.

2.1.2. Cell cultures and transfection

HeLa cells were grown in DMEM high glucose (Euroclone) supplemented with 10% fetal bovine serum (GIBCO), 100 U/ml penicillin (Euroclone) and 100 µg/ml streptomycin (Euroclone). Before transfection, cells were seeded onto 13-mm glass coverslips (immunofluorescence and ER Ca^{2+}) or 6-multiwell plates (western blot and cytosolic Ca^{2+}) and allowed to grow to 70–80% confluence. Transfection was carried out with the Ca^{2+} phosphate procedure, using 4 µg of total DNA for each 13 mm glass coverslip and 12 µg for each well of the 6-multiwell plate. For Ca^{2+} measurement cells were co-transfected with aequorin constructs targeted to different cell compartments (cytAEQ, erAEQ) and pcDNA3 empty vector or short/long PMCA2 wild type/mutated plasmids.

2.1.3. Western blotting analysis

Forty-eight hours after transfection, HeLa cells lysates were quantified by the Bradford assay (Bio-Rad), loaded on an 8% SDS/PAGE Tris-HCl polyacrylamide gel and blotted onto Immobilon-P^{SQ} PVDF Membrane (Merck Millipore). The membrane was blocked for 1 h at room temperature using 5% non-fat dried milk (NFDM) in TBST (20 mM Tris-HCl, pH 7.4, 150 mM NaCl, 0.05% Tween-20) and incubated overnight with the specific primary antibody at 4 °C. Monoclonal anti-PMCA clone 5F10, 1:1000 (Thermo Scientific) and monoclonal anti-β-actin, 1:30000 (Sigma) primary antibodies were used. Detection was carried out by incubation with secondary horseradish peroxidase-conjugated anti-mouse or anti-rabbit IgG antibodies (Santa Cruz Biotechnology) for 1 h at room temperature followed by incubation with the chemiluminescent reagent Luminata HRP substrate (Merck Millipore).

2.1.4. Immunocytochemistry analysis

Forty-eight hours after transfection, HeLa cells were processed for immunofluorescence. The cells were washed twice with phosphate-buffered saline (PBS: 140 mM NaCl, 2 mM KCl, 1.5 mM KH_2PO_4, 8 mM Na_2HPO_4 pH 7.4) and fixed for 20 min with 3,7% formaldehyde in PBS. Cells permeabilization was performed by 20 min incubation with 0,1% Triton X-100 in PBS, followed by 30 min wash with 1% gelatin (type IV, from calf skin, Sigma) in PBS. The coverslips were then incubated for 60 min at 37 °C in a wet chamber with a mouse monoclonal anti-PMCA antibody, 1:20 (Thermo Scientific) in PBS. Staining was revealed by the incubation with specific AlexaFluor488-labeled anti-mouse secondary antibody, 1:50 (Life Technologies) for 45 min at room temperature. Fluorescence was detected with a Leica SP5 confocal microscope and analyzed by ImageJ software.

2.1.5. Aequorin Ca^{2+} measurements

Cytosolic and ER Ca^{2+} measurements were carried out on a PerkinElmer EnVision plate reader equipped with a two-injector unit as previously reported (Vicario et al., 2017).

2.1.6. Peptide synthesis

Wt and mutant C28 peptides corresponding to the 28-residues of PMCA2 z/a and z/b isoforms CaM-BD, were synthesized by automatic

solid phase procedures as previously described (Cali et al., 2017). The sequences of the wt and the mutated peptides, which carried a V or a F residue at position 1143 were the following: PMCA2 z/a LRRGQILWFRGLNRIQTQIKV(F)VKAFRSS; and PMCA2 z/b LRRGQILWFRGLNRIQTQIEV(F)VNTFKSG.

2.1.7. Surface plasmon resonance assay

For SPR analysis, a Biacore™ T100 (GE Healthcare) system was used. PMCA peptides were immobilized on a CM5 (series S) sensor chip (carboxymethylated dextran surface) to a final density of 1200 resonance units (RU), following the amino-coupling method; a 10 mM acetate, pH 5.0 buffer was used for the immobilization. A flow cell with no immobilized peptide was used as control. Binding analyses were carried out as described in (Cali et al., 2017). The curves were fitted with the classical Langmuir 1:1 model or with a two-state binding model; the quality of the fits was assessed by visual inspection of the fitted data and their residual, and by chi-squared values. Although the K_D values calculated with the two models were very similar, better fits were generated by the two-state reaction model.

2.1.8. Molecular dynamics

Initial configurations for the four different MD simulations were obtained starting from the atomic coordinates of the crystal structure of the complex of CaM (with four Ca2 + bound to the EF domains) and the PMCA2 CaM-BD (Juranic et al., 2010). To match the sequence of PMCA2 a/z and z/b and their V1143F mutants, residues were modified using Coot (Emsley et al., 2010). The dynamic of the four systems were performed for 300 ns as previously reported in (Vicario et al., 2017).

2.1.9. Statistical analysis

All of the data are representative of at least three independent experiments unless otherwise indicated. Values are expressed as mean ± SEM. Statistical significance was determined using the Student's *t*-test. A p value ≤ 0.01 was considered statistically significant.

3. Results

3.1. Clinical description of the patient and identification of ATP2B2 mutation

This 27-year-old man, born at term to healthy non-consanguineous parents, presented delayed motor development requesting clinical attention at age 5 months. As a child, he could sit unaided at age 1 year, stand with support at age 2.3, had dysmetria and intentional tremor at age 3 and showed obvious gait ataxia at age 4. While in primary school, his teachers first reported impaired speech and moderate intellectual disability. Over the years his clinical status has been largely stable. At last examination, he was still able to walk, though presented gait and trunk ataxia, had dysarthric speech and hyporeflexia in all limbs. Audiometric testing showed normal results. Metabolic and urine workups were repeatedly normal. Brain MRI studies revealed global cerebellar atrophy without cortical and brainstem involvement (Fig. 1A and B). The patient carried a heterozygous c.3427G > T (p.V1143F) mutation in *ATP2B2* (Fig. 1C), not present in ExAC database of 60,706 control individuals, or in ClinVar. No variants were found in *CDH23*.

3.2. The V1143F mutation impairs the Ca^{2+} handling activity of the short and long PMCA2 isoforms without affecting their expression and plasma membrane localization

To explore the effect of the V1143F replacement on PMCA2 ability to export Ca^{2+}, the vectors encoding the wt and mutant pumps were transfected in HeLa cells and the expression levels were determined by Western blot analysis. Two splicing variants were taken into account, the full-length (*b*) variant (PMCA2 z/b) and the C-terminally truncated splice (*a*) variant (PMCA2 z/a). As shown in Fig. 1D by probing the membrane with an anti-PMCA monoclonal antibody (5F10) recognizing all the pump isoforms, we were able to detect specific bands at the expected molecular weight of about 130 kDa. The V1143F mutant pumps are expressed to the same extent of their wt counterpart. The subcellular localization of the overexpressed pumps was assessed by immunocytochemistry using the 5F10 antibody. Fig. 1E shows that the distribution of the pump was not affected by the mutation and all the overexpressed variants showed specific enrichment at the plasma membrane (inset Fig. 1E). To explore the effect of the V1143F replacement on Ca^{2+} export by the PMCA2 pump, HeLa cells were transfected with the wt or the mutant *a* and *b* pump variants along with a vector encoding the cytosolic Ca^{2+} sensing photoprotein aequorin (cytAEQ), and stimulated with the $InsP_3$-linked agonist histamine (100 μM) to induce Ca^{2+} release from the ER and subsequent Ca^{2+} influx from the extracellular ambient. As shown and quantified in Fig. 2 A and B, cells overexpressing either the *a* or the *b* PMCA2 variants had enhanced ability to clear the histamine-induced Ca^{2+} transient with respect to control cells transfected with cytAEQ alone (peak values: 2,67 ± 0,07, n = 35 for control cells; 1,83 ± 0,05, n = 36 for wt PMCA2 z/a; 1,98 ± 0,04, n = 36 for wt PMCA2 z/b). HeLa cells overexpressing the V1143F mutant pump still displayed a reduced amplitude of the Ca^{2+} peak, indicating that the activity of the pump was not completely abolished by the mutation. However, the amplitude of the peaks reached in the presence of mutant PMCA2 z/a and z/b variants was significantly higher compared to those of the cells overexpressing wt pumps (peaks values: 2,30 ± 0,06, n = 34 for V1143F PMCA2 z/a; 2,32 ± 0,05, n = 36 for V1143F PMCA2 z/b), indicating that the activity of mutant pumps was indeed compromised.

We have previously shown that the overexpression of the PMCA pumps significantly affect the basal ER Ca^{2+} content possibly because of its involvement in shaping the ER Ca^{2+} refilling during the SOCE (Brini et al., 2000; Paszty et al., 2015; Zanni et al., 2012). The monitoring of ER Ca^{2+} levels is thus an important parameter to evaluate PMCA pump activity. For this reason, we assessed the effect of mutant PMCA2 expression on ER Ca^{2+} levels. To this aim the free $[Ca^{2+}]$ in the ER lumen was measured by expressing the ER targeted low affinity variant of the photoprotein aequorin (erAEQ) in HeLa cells either alone or together with the wt or the mutated PMCA2 pump *a* and *b* variants. As shown and quantified in Fig. 2C and D, in agreement with previous reports (Brini et al., 2000; Zanni et al., 2012), the maximum $[Ca^{2+}]_{ER}$ reached in control cells was significantly higher than in those observed in cell overexpressing the PMCA2 z/a pumps (Fig. 2C, plateau value: 245,70 ± 15,74 μM, n = 12 for control cells; 126 ± 5,86 μM, n = 10 for the wt PMCA2 z/a pump; 176,13 ± 10,98 μM, n = 10 for the V1143F PMCA2 z/a pump), or the PMCA2 z/b pumps (Fig. 2D, plateau value: 245,70 ± 15,74 μM, n = 12 for control cells; 105,56 ± 3,83 μM, n = 10 for the wt PMCA2 z/b pump; 157,90 ± 6,19 μM, n = 9 for the V1143F PMCA2 z/b pump). The finding that the ER Ca^{2+} content was much more reduced in cells overexpressing the wt pump than in those overexpressing the mutant PMCA2 further highlights the occurrence of a defect in the Ca^{2+} extrusion ability of the mutant pump that possibly results in the increased availability of cytosolic Ca^{2+} to be pumped in the ER lumen by the SERCA pump.

3.3. Effect of the V1143F mutation on the response of the PMCA2 pump to the Ca^{2+} released from the ER and to the Ca^{2+} entered from the extracellular ambient

The Ca^{2+} transients generated by histamine stimulation in the presence of physiological concentrations of extracellular Ca^{2+} (1 mM $CaCl_2$) are due to the Ca^{2+} released from the intracellular stores (ER and Golgi) and the Ca^{2+} influx from the external milieu through the store-operated Ca^{2+} channels activated by the emptying of the stores (SOCE). To better evaluate the Ca^{2+} extrusion ability of the PMCA

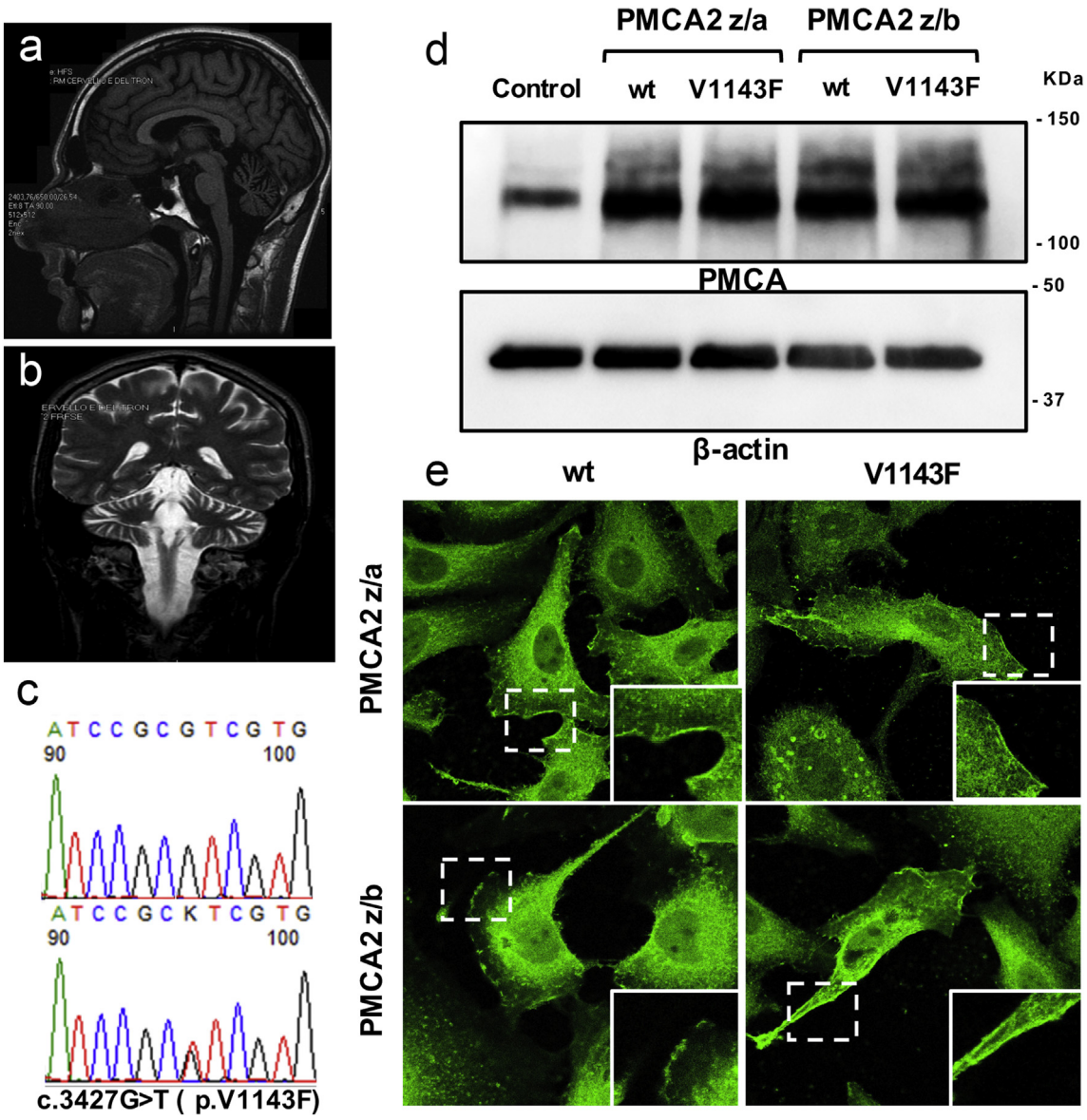

Fig. 1. Neuroimaging and sequencing analysis of the patient and study of the expression and localization of exogenous PMCA2 in HeLa cells. T1 weighted mid-sagittal section (A) and T2 weighted coronal section (B) of the patients at the age of 22 years, showing global cerebellar atrophy without cortical and brainstem involvement. C) Sanger sequencing chromatograms in the patient (upper panel) and a control (lower panel). Western blotting (D) and immunocytochemistry (E) analysis showing the expression level and intracellular localization of the wild type and mutated truncated and full-length PMCA2. The pump was revealed by the monoclonal mouse antibody 5F10.

pump we decided to separately analyze these two components: cytosolic Ca^{2+} transients were first monitored in cells stimulated with histamine in the absence of extracellular Ca^{2+} (in the Krebs–Ringer buffer (KRB) supplemented with 100 μM EGTA), and then upon Ca^{2+} re-addition. In the absence of extracellular Ca^{2+}, thus, the transients were only shaped by the release of Ca^{2+} from the intracellular stores. As shown and quantified in Fig. 3A and B, the overexpression of either the wt or the mutated pumps reduced the amplitude of the peak. Nevertheless, the extent of the reduction was smaller than further in cells expressing the V1143F mutant pumps, indicating that the latter were significantly compromised in their Ca^{2+} extrusion ability (peaks values: 1,76 ± 0,08, n = 32 for control cells; 0,55 ± 0,03, n = 23 for the wt z/a pump; 0,71 ± 0,05, n = 24 for the mutant z/a PMCA2; 0,56 ± 0,03, n = 23 for the wt z/b pump; 0,75 ± 0,06, n = 27 for the mutant z/b PMCA2). Considering the strong phenotype observed in Fig. 2C and D, the differences observed here were expected to be much higher if they had only been dependent and/or directly linked to the free ER Ca^{2+} content, thus suggesting that the intrinsic ability of the PMCA2 to pump Ca^{2+} to the extracellular medium was compromised by the mutation. To gain further insights on this point, in a second approach the intracellular Ca^{2+} deposits were pre-depleted by treating cells for 5 min with the SERCA inhibitor thapsigargin in the presence of histamine in a KRB buffer containing 1 mM EGTA. Under these conditions, the addition of a KRB solution containing 3 mM $CaCl_2$ to the cells would induce the sudden increase of Ca^{2+} entry from the extracellular ambient. As shown and quantified in Fig. 3C and D the height of the peak generated under these conditions, which reflected the magnitude of Ca^{2+} influx, was higher than that obtained upon histamine stimulation in the presence of extracellular Ca^{2+} (Fig. 2A and B), and was not affected by the overexpression of either the wt or the mutated pumps. This suggests that under these conditions the activity of the PMCA pumps could be overwhelmed/hidden by that of the much powerful Ca^{2+} influx channels and thus no effects on the height and the decline of the peak transients both in the case of wt and mutant pumps becomes

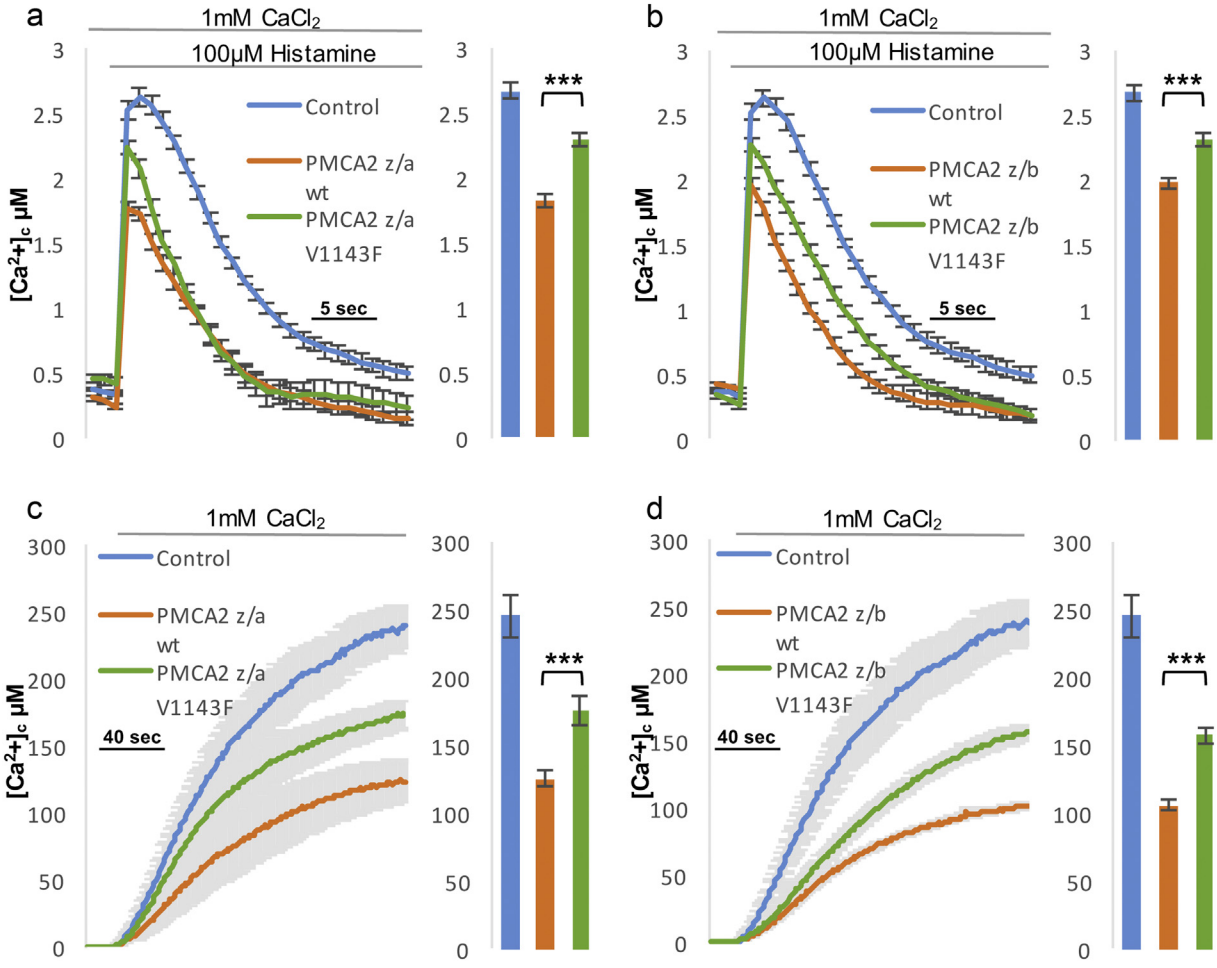

Fig. 2. Effect of the short and long wt and mutant pumps expression on cytosolic Ca^{2+} transient and ER Ca^{2+} influx. (A and B) Cytosolic Ca^{2+} transients and average peak values recorded following 100 μM histamine stimulation of HeLa cells overexpressing the cytAEQ either alone or along with the wt or the V1143F mutant PMCA2 z/a or z/b pump. (C and D) HeLa cells were cotransfected with erAEQ and the PMCA2 constructs or transfected with erAEQ only. Traces of the ER Ca^{2+} influx upon re-addiction of 2 mM Ca^{2+} after Ca^{2+} store depletion are shown. Bars represent mean $[Ca^{2+}]$ values upon stimulation (μM ± SEM). ***, $p < 0{,}0001$.

appreciable. Intriguingly, as the Ca^{2+} peaks declined, a plateau was reached (Fig. 3E and F) at about 1.5 μM Ca^{2+} in control cells: at this cytosolic Ca^{2+} threshold the ability of the pump to extrude Ca^{2+} became appreciable. A different behavior for the two splicing variants was observed, the z/b variant being much more effective than the z/a pump, as previously shown (Ficarella et al., 2007). In the case of the C-terminally truncated *a* variant, cytosolic plateau levels were similar in cells overexpressing the wt and the mutated pump, whereas in those expressing the full-length *b* variant, the levels attained when the mutated pump was present were significantly higher than in those attained in the case of wt PMCA2 pump (Fig. 3E and F), suggesting that under those conditions the V1143F mutation compromised the activity of the full-length *b* variant more severely than the truncated *a* variant. These differences between the *a* and the *b* variants of the pump convinced us to evaluate whether the mutation had an impact on the CaM-BD ability to interact with the main core of the pump (the process of auto-inhibition) and on its interplay with CaM as well. Thus, the basal auto-inhibition of the pump (*i.e.* in absence of Ca^{2+}/CaM) was evaluated by a well-established yeast functional complementation assay in K616 cells (Cali et al., 2015; Ton and Rao, 2004; Vicario et al., 2017). As shown in Supplementary Figure 1 independent clones of yeast K616 cells expressing either the wild-type or the V1143F mutant of the PMCA2 pumps (z/a and z/b isoforms) were selected, and the viability and growth rates of yeast cells were checked both in a Ca^{2+}-free non-permissive medium, and in a Ca^{2+}-containing permissive medium. Western Blot analysis confirmed that the yeast cells expressed comparable levels of exogenous proteins (Supplementary Figure 1B), but no differences were found in the growth of the cells expressing the wt or the mutated *a* and *b* variants: suggesting that, at variance with what was observed for the G1107D mutation in the CaM-BD of the PMCA3 isoform (Cali et al., 2016), this mutation did not significantly affect the basal auto-inhibition of the pump.

3.4. *In silico molecular dynamic simulations and in vitro surface plasmon resonance (SPR) analysis of the interplay of CaM with the synthetic CaM-BD of PMCA2 z/a and PMCA2 z/b*

Having ruled out a detrimental effect of the V1143F mutation on the ability of the PMCA2 CaM-BD to mediate the basal auto-inhibition of the pump, we decided to perform an *in silico* and *in vitro* analysis of the interplay of CaM with the wt and mutated CaM-BD of both the *a* and the *b* variants of the PMCA2 pump.

A series of molecular dynamic simulations was first performed to explore the interplay of CaM with the wt and the mutated domains of the *a* and the *b* variants of the pump molecularly. As shown in Fig. 4A–D, in the simulation model CaM is wrapped around the wt CaM-BD of either the *a* and the *b* variant. V1143 resides in proximity of Phe68 of CaM for the whole duration of the simulation (300 ns). Moreover, the trajectories in both variants appear consistent with each other and evolve towards two similar final configurations (Supplementary Figure 2). By contrast, the replacement of V1143 with a bulkier Phe residue (which, evidently, cannot be accommodated in the

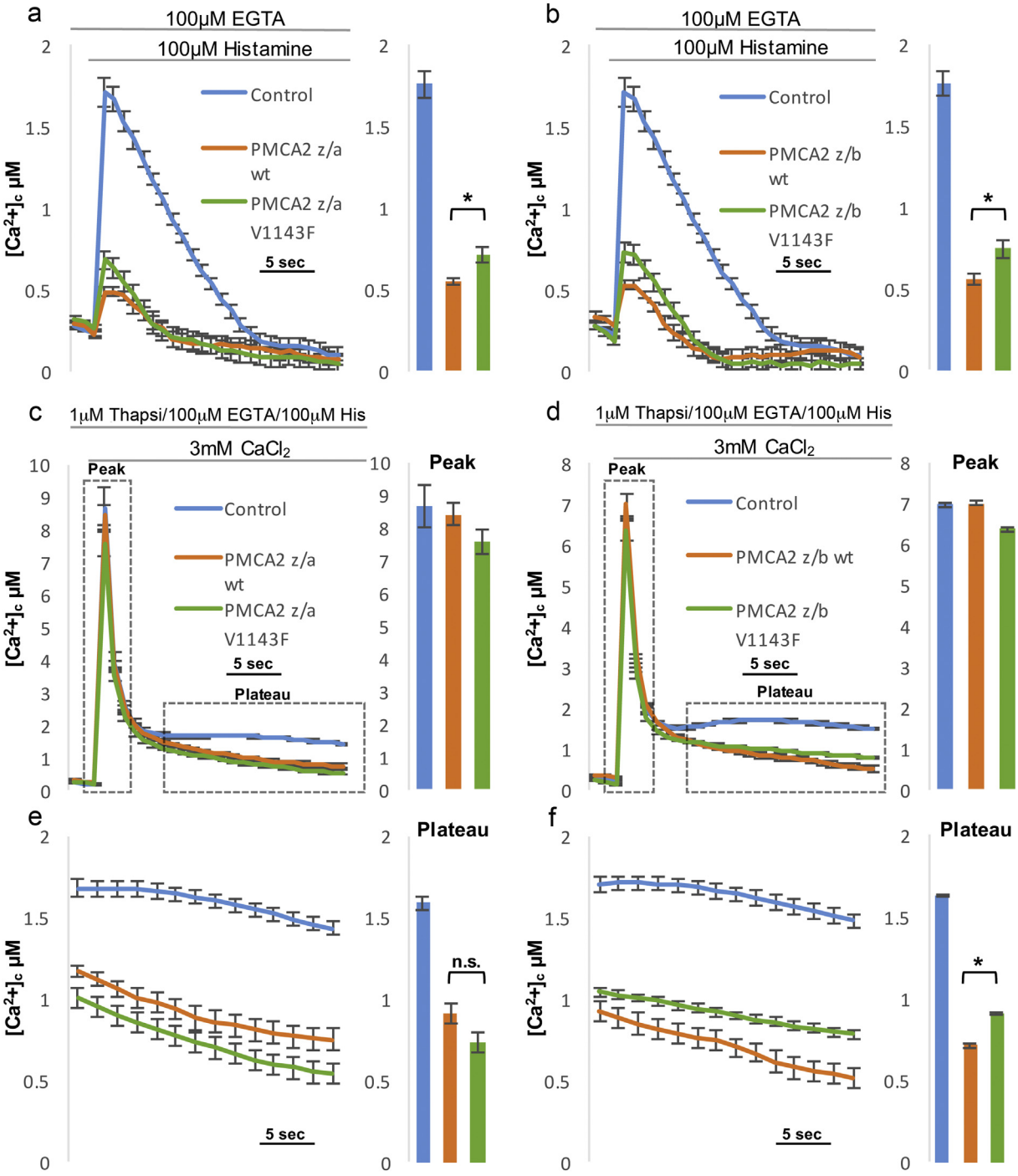

Fig. 3. Effect of the short and long wt and mutant pumps expression on Ca^{2+} released from the ER and on Ca^{2+} influx from the extracellular ambient. HeLa cells were cotransfected with cytAEQ and the PMCA2 constructs, or transfected with cytAEQ only and stimulated with histamine 100 μM in the absence of extracellular Ca^{2+} (100 μM EGTA) (A–B) or pre-treated with 1 μM thapsigargin and 100 μM histamine in a buffer containing 1 mM EGTA for 5 min and perfused in the presence of KRB supplemented with 3 mM Ca^{2+} to stimulate Ca^{2+} entry from the extracellular ambient (C–D). Cytosolic Ca^{2+} transients and mean $[Ca^{2+}]$ values upon stimulation are shown in panels A–D. Enlargements of the peaks decay before reaching the plateau phase and $[Ca^{2+}]$ at the plateau are shown in panels E and F. *$p < 0,01$.

space occupied by Val), forces a rearrangement of the CaM-BD helixes in the two mutants (Fig. 4C and D), producing local strains which bend (isoform z/a) or partially unfold (isoform z/b) the two CaM-BD helixes, indicating that the two mutated domains are less adequate for the proper interaction with CaM. In agreement with this observation, the RMSD shows higher value and longer equilibration times for the mutants than their wt counterparts (Supplementary Figure 3).

Lastly, to corroborate the results shown above, the wt and the mutated peptides corresponding to the CaM-BD were synthesized, immobilized on the chip surface and perfused with 0.25 μM CaM in the presence of 5 mM $CaCl_2$. Then, the wt and the mutated peptides immobilized on the chip surface were perfused with increasing concentrations of CaM in the presence of 5 mM $CaCl_2$. The resulting typical sensorgrams displaying the bimodal kinetic of binding composed by a rising and a decay phase indicative of the association (k_{on}) and dissociation (k_{off}) of CaM with and from its CaM-BD, respectively, are shown in Fig. 5A–D. Interestingly (and in line with what observed in Fig. 3C–F), the synthetic peptides corresponding to the truncated *a*

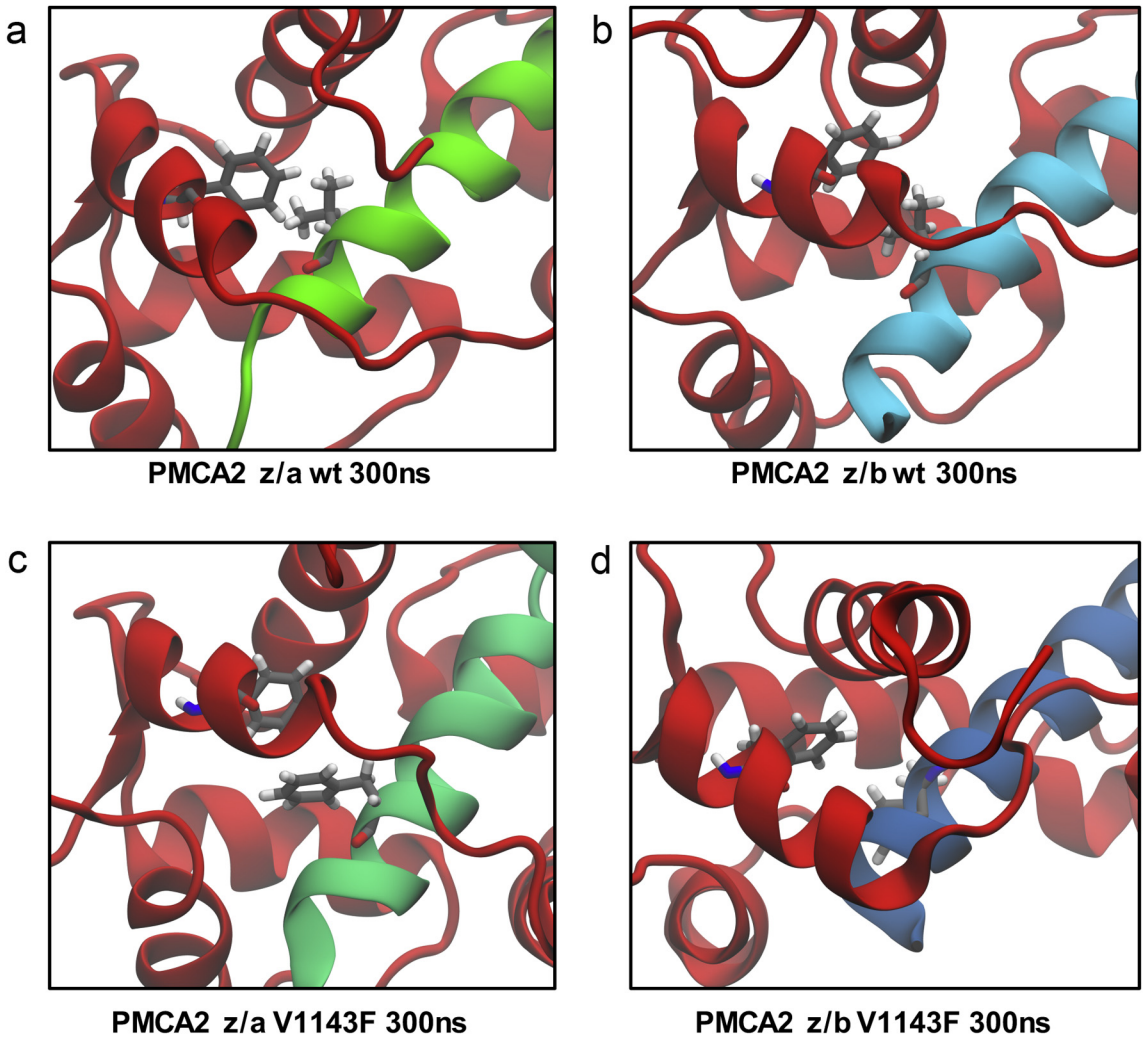

Fig. 4. Molecular modelling of the interaction between CaM and its binding domain in the PMCA2 z/a and z/b pumps. Detailed view of the Val1143 residues of the wild type PMCA2 z/a (light green, panel A) and PMCA2 z/b (light blue, panel B) and of the Phe1143 residues of the mutated PMCA2 z/a (dark green, panel C) and PMCA2 z/b (dark blue, panel D) in proximity to Phe68 of the CaM (red). (For interpretation of the references to colour in this figure legend, the reader is referred to the web version of this article.)

variant behaved differently from those corresponding to the full-length *b* variant: in the former the mutation impacted on the dissociation rate of the CaM (*i.e.*, a faster k_{off}, was detected) while the affinity for CaM was essentially unaffected (indicative of the fact that the mutated domain was less able to maintain the CaM bound); in the latter a decreased k_{on} and an increased k_{off} were observed (indicative of the fact that both the association and the dissociation are affected) and the affinity for CaM in the mutated peptide was reduced (Table 1). The experiments show that the mutation selectively decreased the affinity of the pump for CaM, but the effect was not appreciable in the C-terminally truncated *a* variant of the pump.

4. Conclusions

Cerebellar ataxias are rare neurological disorders whose main symptoms are the lack of voluntary coordination of muscle movements and gait abnormality (Manto and Marmolino, 2009). Inherited cerebellar ataxias derive from alterations of cerebellar structures or a combination of cerebellar and extra-cerebellar lesions and are generally classified as autosomal recessive, autosomal dominant or X-linked recessive (Manto and Marmolino, 2009). Different mutations have been associated with inherited cerebellar ataxias, among them those of oligophrenin-1 (OPHN1) (36–38) and calcium/calmodulin-dependent protein kinase (CASK) (Najm et al., 2008). As mentioned in the Introduction, mutations of the PMCA3 pump have also been associated with cerebellar ataxias. As a rule, neurons express all 4 PMCA isoforms, but, at variance with other human tissues, in neurons PMCA2 and PMCA3 tend to predominate (Brini and Carafoli, 2009). The reasons for the predominance are not obvious, but are likely to be due to differences in function that are supposedly not essential: two of them, however, may be significant. They are the higher affinity of these two isoforms for the classical activator calmodulin and their peculiar ability to function efficiently also in the absence of calmodulin (Brini and Carafoli, 2009; Stafford et al., 2017). One could for instance guess that the special importance of Ca^{2+} signaling to neurons would demand that the PMCA pumps function more or less continuously irrespective of the presence of calmodulin, and, similarly, that they would be better able to interact with calmodulin that he ubiquitous isoforms. PMCA2 and 3 accumulate in the synaptic region of the molecular layer of the cerebellar cortex, the brain region involved in motor control and sensory perception, mainly constituted by Purkinje neurons (Burette and Weinberg, 2007). Noteworthy, PMCA2 is predominantly postsynaptic, while PMCA3 distributes mainly at the presynaptic level, suggesting specific roles for the two isoforms (Burette and Weinberg, 2007). At synapses, PMCAs also control the release of neurotransmitters (Roome and Empson, 2010, 2013; Roome et al., 2013).

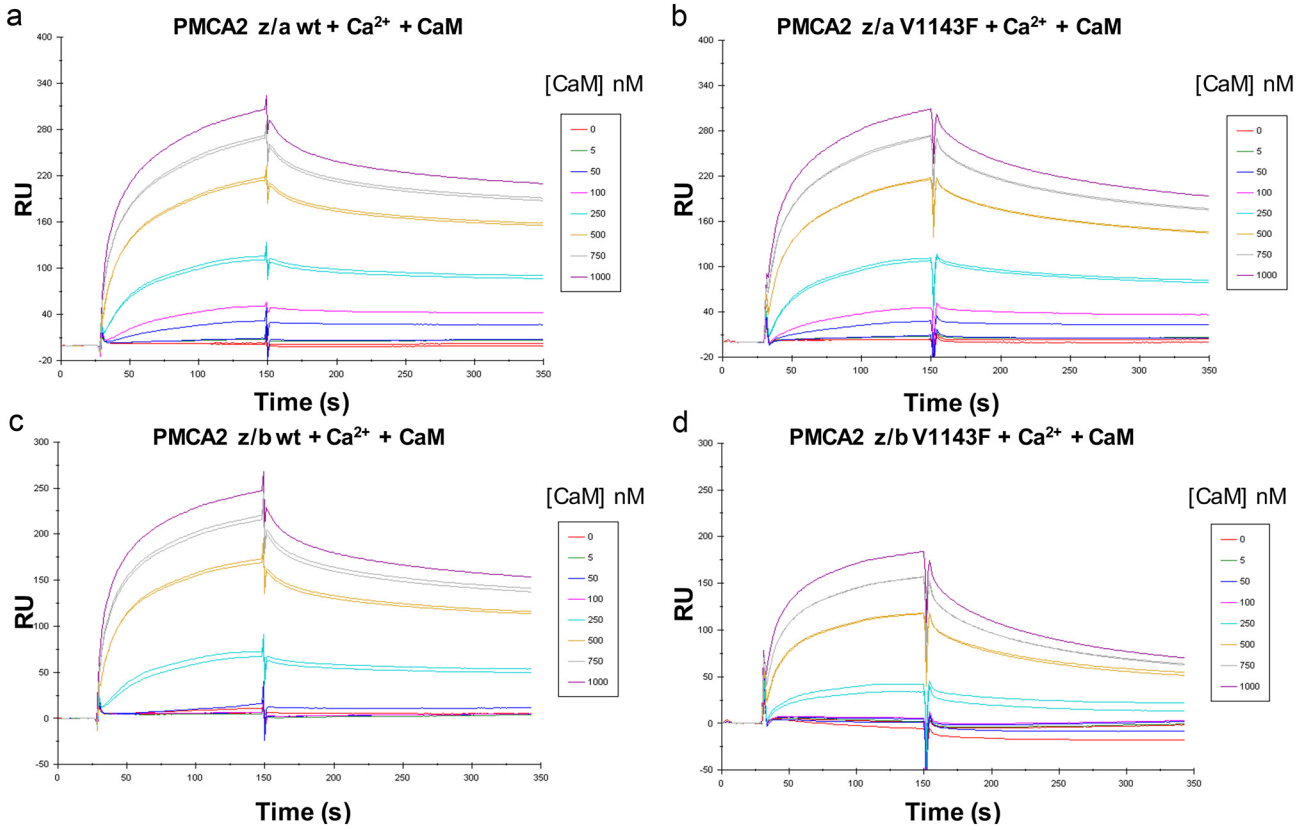

Fig. 5. SPR analysis of the interaction between CaM and its binding domain in the PMCA2 z/a and z/b pumps. Representative sensorgrams (time-course of the surface plasmon resonance signal) for the interaction of CaM to its binding domain. The CaM-BD peptides (A and C, wt; B and D, V1143F mutants) were immobilized on the chip surface while CaM was injected in the solution, in the presence of 5 mM $CaCl_2$, and flowed over the surface at the indicated concentrations. RU, resonance units.

Table 1
Kinetic parameters of the interaction between CaM and its binding domain on PMCA2 z/a and z/b pumps: the K_{on}, K_{off} and K_D of the interaction between CaM and its binding domain on PMCA2 z/a and z/b pumps. Values are expressed as mean ± SEM.

		k_{on} ($M^{-1} s^{-1}$)	k_{off} (s^{-1})	K_D (nM)
PMCA2	wt	z/a: $1.6 \times 10^4 \pm 1.6 \times 10^2$	z/a: $8.8 \times 10^{-4} \pm 8.5 \times 10^{-5}$	z/a: 54 ± 3.0
		z/b: $2.1 \times 10^4 \pm 7.1 \times 10^2$	z/b: $1.4 \times 10^{-3} \pm 4.7 \times 10^{-5}$	z/b: 69 ± 1.4
	V1143F	z/a: $1.5 \times 10^4 \pm 1.8 \times 10^2$	z/a: $1.3 \times 10^{-3} \pm 2.3 \times 10^{-5}$	z/a: 82 ± 2.4
		z/b: $1.6 \times 10^4 \pm 3.4 \times 10^2$	z/b: $2.1 \times 10^{-3} \pm 3.6 \times 10^{-5}$	z/b: 135 ± 5.1

As mentioned, the link between PMCA3 mutations and X-linked cerebellar ataxia has now been repeatedly described (Cali et al., 2015; Feyma et al., 2016; Vicario et al., 2017; Zanni et al., 2012). The other neuronal-enriched pump isoform, PMCA2, is also important to cerebellar functions: it is highly expressed in Purkinje neurons (Filoteo et al., 1997; Hillman et al., 1996) where it helps clearing Ca^{2+} transients generated by stimulation and cooperates in the control of basal Ca^{2+} concentration (Empson et al., 2010b; Ueno et al., 2002); its Ca^{2+} extrusion activity also helps regulating the frequency and amplitude of spontaneous inhibitory post-synaptic currents of the molecular layer interneurons (Empson et al., 2013) as well as their dendritic growth (Empson et al., 2010a; Sherkhane and Kapfhammer, 2013). In the mutations or deletion of the PMCA2 pump linked to hearing loss phenotypes in mice and humans (Bortolozzi et al., 2010; Ficarella et al., 2007; Kozel et al., 1998; Schultz et al., 2005; Spiden et al., 2008; Street et al., 1998; Takahashi and Kitamura, 1999; Tsai et al., 2006; Wood et al., 2004), hearing loss has been considered the most important consequence of the mutations: a reasonable suggestion, as the PMCA2 pump is the only means to eject Ca^{2+} from the stereocilia of outer hair cells of the Corti organ. Intriguingly, however, an ataxic-like behavior has also been described in PMCA2 null mice and in the deaf *Wriggle mouse sagami* (Kozel et al., 1998; Ueno et al., 2002). Whether these disturbances are related to the deafness phenotype or directly linked to cerebellar dysfunctions is still unknown. In mice, particularly severe PMCA2 mutations could be sufficient to induce the deafness phenotype (Spiden et al., 2008), but in other mouse mutations, and in the human mutations (Ficarella et al., 2007; Schultz et al., 2005), the concomitant mutation in the stereociliar Ca^{2+} binding protein cadherin 23 suggests the intriguing possibility that PMCA2 dysfunctions might only aggravate the deafness phenotype, which would have the cadherin 23 mutation as the principal causative factor, while being primarily responsible for the ataxic phenotype. In line with this observation, heterozygotes *deafwaddler* as well as heterozygous PMCA2 knock-out mice show a milder ataxic phenotype than the homozygous mice, indicating a link between ataxia manifestation and the PMCA2 gene dosage (Empson et al., 2010b; McCullough and Tempel, 2004). The presence of additional mutations in other proteins has actually been a constant also in the cases of cerebellar ataxias associated to PMCA3 defects (Cali et al., 2015; Vicario et al., 2017).

In this study, we have described the effects of a novel missense mutation (V1143F) in the CaM-BD of the neuron-enriched isoform 2 of the PMCA pump of a human patient suffering from congenital

cerebellar ataxia. To the best of our knowledge this is the first PMCA2 mutation over a cadherin 23 wt background in a subject with the hearing ability fully retained. Although segregation analysis could not be performed due to lack of consent from the parents, thus raising the possibility that additional mutation may have caused the ataxia in this patient, the finding that such PMCA2 mutation is not present in ExAC database of 60,706 control individuals, or in ClinVar strongly supports its pivotal role in the cerebellar dysfunction.

The V1143F substitution did not alter the expression level of the PMCA2 pump nor its targeting to the plasma membrane, but compromised its Ca^{2+} pumping function, without impacting on its basal autoinhibited state (Enyedi et al., 1989). *In vitro* surface plasmon resonance work and *in silico* molecular dynamic simulations of CaM binding to its CaM-BD have demonstrated that the interplay of the mutated CaM-BD with CaM was compromised, the effect being particularly significant in the full-length *b* variant of the pump. The prolonged duration of the Ca^{2+} transients induced by cell stimulation in cells expressing the mutated pump have documented its inability to maintain the correct Ca^{2+} homeostasis within neurons. These findings, and the results of the molecular dynamics simulations, have thus defined and characterized the phenomenology of the ataxia-associated PMCA2 pump defect. At the present stage of development, the fine molecular mechanism(s) by which the deficient pump function is eventually translated in the generation of the ataxic phenotype is still not understood. One last comment that is possibly related to the last statement is in order at this point: the functional pump defect caused by the mutation did not appear to be of particularly gravity. However, the experimental protocol by necessity explored the effect on the global homeostasis of Ca^{2+}. As mentioned repeatedly, the PMCA pumps only offer a minor contribution to it, their main role being the regulation of Ca^{2+} signaling in selective sub-plasma membrane microdomains that host signaling pump partners of central importance to cell function. It is felt that future work on this selective Ca^{2+} signaling cellular (neuronal) microcosmos, that would include the development of currently unavailable experimental protocols, could possibly shed light on the link between PMCA pump defects and the ataxic phenotype.

Supplementary data to this article can be found online at https://doi.org/10.1016/j.nbd.2018.04.009.

Acknowledgments

This research was supported by grants from the Ministry of University and Research (Bando SIR 2014 no. RBSI14C65Z to T.C.) and from the University of Padova (Progetto Giovani 2012 no. GRIC128SP0 to T.C., Progetto di Ateneo 2016 no. CALI_SID16_01 to T.C., Progetto di Ateneo 2015 no. CPDA153402 to M.B.). Ministry of Health (Ricerca Finalizzata grant NET-2013-02356160 to EB). We thank Dr. S. Barresi and Dr. C. Passarelli (Unit of Medical Genetics, B. Gesù Children's Hospital) for technical support in genetic screening.

Conflict of interest

The authors declare no conflict of interest.

References

Bortolozzi, M., et al., 2010. The novel PMCA2 pump mutation Tommy impairs cytosolic calcium clearance in hair cells and links to deafness in mice. J. Biol. Chem. 285, 37693–37703.
Brini, M., Carafoli, E., 2009. Calcium pumps in health and disease. Physiol. Rev. 89, 1341–1378.
Brini, M., et al., 2000. Effects of PMCA and SERCA pump overexpression on the kinetics of cell Ca(2+) signalling. EMBO J. 19, 4926–4935.
Burette, A., Weinberg, R.J., 2007. Perisynaptic organization of plasma membrane calcium pumps in cerebellar cortex. J. Comp. Neurol. 500, 1127–1135.
Cali, T., et al., 2015. A novel mutation in isoform 3 of the plasma membrane Ca2+ pump impairs cellular Ca2+ homeostasis in a patient with cerebellar ataxia and laminin subunit 1alpha mutations. J. Biol. Chem. 290, 16132–16141.
Cali, T., et al., 2016. The ataxia related G1107D mutation of the plasma membrane Ca2+ ATPase isoform 3 affects its interplay with calmodulin and the autoinhibition process. Biochim. Biophys. Acta 1863, 165–173.
Cali, T., et al., 2017. The ataxia related G1107D mutation of the plasma membrane Ca2+ ATPase isoform 3 affects its interplay with calmodulin and the autoinhibition process. Biochim. Biophys. Acta 1863, 165–173.
Carafoli, E., 1994. Biogenesis: plasma membrane calcium ATPase: 15 years of work on the purified enzyme. FASEB J. 8, 993–1002.
Dumont, R.A., et al., 2001. Plasma membrane Ca2+-ATPase isoform 2a is the PMCA of hair bundles. J. Neurosci. 21, 5066–5078.
Eakin, T.J., et al., 1995. Localization of the plasma membrane Ca(2+)-ATPase isoform PMCA3 in rat cerebellum, choroid plexus and hippocampus. Brain Res. Mol. Brain Res. 29, 71–80.
Empson, R.M., et al., 2010a. The role of the calcium transporter protein plasma membrane calcium ATPase PMCA2 in cerebellar Purkinje neuron function. Funct. Neurol. 25, 153–158.
Empson, R.M., et al., 2010b. Reduced expression of the Ca(2+) transporter protein PMCA2 slows Ca(2+) dynamics in mouse cerebellar Purkinje neurones and alters the precision of motor coordination. J. Physiol. 588, 907–922.
Empson, R.M., et al., 2013. Enhanced synaptic inhibition in the cerebellar cortex of the ataxic PMCA2(−/−) knockout mouse. Cerebellum 12, 667–675.
Emsley, P., et al., 2010. Features and development of Coot. Acta Crystallogr. D Biol. Crystallogr. 66, 486–501.
Enyedi, A., et al., 1989. The calmodulin binding domain of the plasma membrane Ca2+ pump interacts both with calmodulin and with another part of the pump. J. Biol. Chem. 264, 12313–12321.
Falchetto, R., et al., 1991. The plasma membrane Ca2+ pump contains a site that interacts with its calmodulin-binding domain. J. Biol. Chem. 266, 2930–2936.
Falchetto, R., et al., 1992. The calmodulin-binding site of the plasma membrane Ca2+ pump interacts with the transduction domain of the enzyme. Protein Sci. 1, 1613–1621.
Feyma, T., et al., 2016. Dystonia in ATP2B3-associated X-linked spinocerebellar ataxia. Mov. Disord. 31, 1752–1753.
Ficarella, R., et al., 2007. A functional study of plasma-membrane calcium-pump isoform 2 mutants causing digenic deafness. Proc. Natl. Acad. Sci. U. S. A. 104, 1516–1521.
Figueroa, K.P., et al., 2016. Spontaneous shaker rat mutant - a new model for X-linked tremor/ataxia. Dis. Model. Mech. 9, 553–562.
Filoteo, A.G., et al., 1997. Plasma membrane Ca2+ pump in rat brain. Patterns of alternative splices seen by isoform-specific antibodies. J. Biol. Chem. 272, 23741–23747.
Hillman, D.E., et al., 1996. Ultrastructural localization of the plasmalemmal calcium pump in cerebellar neurons. Neuroscience 72, 315–324.
Juranic, N., et al., 2010. Calmodulin wraps around its binding domain in the plasma membrane Ca2+ pump anchored by a novel 18-1 motif. J. Biol. Chem. 285, 4015–4024.
Kozel, P.J., et al., 1998. Balance and hearing deficits in mice with a null mutation in the gene encoding plasma membrane Ca2+-ATPase isoform 2. J. Biol. Chem. 273, 18693–18696.
Lopreiato, R., et al., 2014. The plasma membrane calcium pump: new ways to look at an old enzyme. J. Biol. Chem. 289, 10261–10268.
Manto, M., Marmolino, D., 2009. Cerebellar ataxias. Curr. Opin. Neurol. 22, 419–429.
McCullough, B.J., Tempel, B.L., 2004. Haplo-insufficiency revealed in deafwaddler mice when tested for hearing loss and ataxia. Hear. Res. 195, 90–102.
Najm, J., et al., 2008. Mutations of CASK cause an X-linked brain malformation phenotype with microcephaly and hypoplasia of the brainstem and cerebellum. Nat. Genet. 40, 1065–1067.
Paszty, K., et al., 2015. Plasma membrane Ca(2)(+)-ATPases can shape the pattern of Ca(2)(+) transients induced by store-operated Ca(2)(+) entry. Sci. Signal. 8, ra19.
Pedersen, P., Carafoli, E., 1987. Ion motive ATPases. I. Ubiquity, properties and significance to cell function. Trends Biochem. Sci. 12, 146–150.
Penheiter, A.R., et al., 2001. Characterization of the deafwaddler mutant of the rat plasma membrane calcium-ATPase 2. Hear. Res. 162, 19–28.
Roome, C.J., Empson, R.M., 2010. Assessment of the contribution of the plasma membrane calcium ATPase, PMCA, calcium transporter to synapse function using patch clamp electrophysiology and fast calcium imaging. Methods Mol. Biol. 637, 343–360.
Roome, C.J., Empson, R.M., 2013. The contribution of the sodium-calcium exchanger (NCX) and plasma membrane Ca(2+) ATPase (PMCA) to cerebellar synapse function. Adv. Exp. Med. Biol. 961, 251–263.
Roome, C.J., et al., 2013. Functional contributions of the plasma membrane calcium ATPase and the sodium-calcium exchanger at mouse parallel fibre to Purkinje neuron synapses. Pflugers Arch. 465, 319–331.
Schultz, J.M., et al., 2005. Modification of human hearing loss by plasma-membrane calcium pump PMCA2. N. Engl. J. Med. 352, 1557–1564.
Sherkhane, P., Kapfhammer, J.P., 2013. The plasma membrane Ca2+-ATPase2 (PMCA2) is involved in the regulation of Purkinje cell dendritic growth in cerebellar organotypic slice cultures. Neural Plast. 2013, 321685.
Spiden, S.L., et al., 2008. The novel mouse mutation Oblivion inactivates the PMCA2 pump and causes progressive hearing loss. PLoS Genet. 4, e1000238.
Stafford, N., et al., 2017. The plasma membrane calcium ATPases and their role as major new players in human disease. Physiol. Rev. 97, 1089–1125.
Stahl, W.L., et al., 1992. Plasma membrane Ca(2+)-ATPase isoforms: distribution of mRNAs in rat brain by in situ hybridization. Brain Res. Mol. Brain Res. 16, 223–231.
Stauffer, T.P., et al., 1997. Immunolocalization of the plasma membrane Ca2+ pump isoforms in the rat brain. Brain Res. 748, 21–29.
Street, V.A., et al., 1998. Mutations in a plasma membrane Ca2+-ATPase gene cause deafness in deafwaddler mice. Nat. Genet. 19 (4), 390.

Strehler, E.E., Zacharias, D.A., 2001. Role of alternative splicing in generating isoform diversity among plasma membrane calcium pumps. Physiol. Rev. 81, 21–50.
Takahashi, K., Kitamura, K., 1999. A point mutation in a plasma membrane Ca(2+)-ATPase gene causes deafness in Wriggle Mouse Sagami. Biochem. Biophys. Res. Commun. 261, 773–778.
Tolosa de Talamoni, N., et al., 1993. Immunocytochemical localization of the plasma membrane calcium pump, calbindin-D28k, and parvalbumin in Purkinje cells of avian and mammalian cerebellum. Proc. Natl. Acad. Sci. U. S. A. 90, 11949–11953.
Ton, V.K., Rao, R., 2004. Functional expression of heterologous proteins in yeast: insights into Ca2+ signaling and Ca2+ −transporting ATPases. Am. J. Physiol. Cell Physiol. 287, C580–9.
Tsai, Y.S., et al., 2006. A de novo deafwaddler mutation of Pmca2 arising in ES cells and hitchhiking with a targeted modification of the Pparg gene. Mamm. Genome 17, 716–722.
Ueno, T., et al., 2002. A mouse with a point mutation in plasma membrane Ca2+-ATPase isoform 2 gene showed the reduced Ca2+ influx in cerebellar neurons. Neurosci. Res. 42, 287–297.
Verma, A.K., et al., 1988. Complete primary structure of a human plasma membrane Ca2+ pump. J. Biol. Chem. 263, 14152–14159.
Vicario, M., et al., 2017. A novel PMCA3 mutation in an ataxic patient with hypomorphic phosphomannomutase 2 (PMM2) heterozygote mutations: biochemical characterization of the pump defect. Biochim. Biophys. Acta 1863, 3303–3312.
Wood, J.D., et al., 2004. Low endolymph calcium concentrations in deafwaddler2J mice suggest that PMCA2 contributes to endolymph calcium maintenance. J. Assoc. Res. Otolaryngol. 5, 99–110.
Zanni, G., et al., 2012. Mutation of plasma membrane Ca2+ ATPase isoform 3 in a family with X-linked congenital cerebellar ataxia impairs Ca2+ homeostasis. Proc. Natl. Acad. Sci. U. S. A. 109, 14514–14519.